Supplementary information for "Efficient quantum simulation of photosynthetic light harvesting"

Bi-Xue Wang,[1,*] Ming-Jie Tao,[2,1,*] Qing Ai,[3,2,*] Tao Xin,[1] Neill Lambert,[3] Dong Ruan,[1]
Yuan-Chung Cheng,[4] Franco Nori,[3,5] Fu-Guo Deng,[2,6,†] and Gui-Lu Long[1,7,8,9,10,‡]

[1]*State Key Lab for Low-dimensional Quantum Physics and Department of Physics, Tsinghua University, Beijing 100084*
[2]*Department of Physics, Applied Optics Beijing Area Major Laboratory, Beijing Normal University, Beijing 100875*
[3]*Theoretical Quantum Physics Laboratory, RIKEN Cluster for Pioneering Research, Wako-shi, Saitama 351-0198*
[4]*Department of Chemistry, National Taiwan University, Taipei City 106*
[5]*Physics Department, The University of Michigan, Ann Arbor, Michigan 48109-1040*
[6]*NAAM-Research Group, Department of Mathematics, Faculty of Science, King Abdulaziz University, Jeddah 21589*
[7]*Beijing National Research Center on Information Science and Technology, Beijing 100084*
[8]*School of Information Science and Technology, Tsinghua University, Beijing 100084*
[9]*Innovation Center of Quantum Matter, Beijing 100084*
[10]*Beijing Academy of Quantum Information, Beijing 100085*

CONTENTS

* These authors contributed equally to this work
† fgdeng@bnu.edu.cn
‡ gllong@tsinghua.edu.cn

1. RAMSEY-LIKE DYNAMICS IN PHOTOSYNTHESIS

In this section, we provide a detailed derivation for the Ramsey-like dynamics in photosynthesis [S1, S2]. We assume the total Hamiltonian to be

$$H=\varepsilon_D|1\rangle\langle 1|+\varepsilon_A|2\rangle\langle 2|+\sum_k\omega_k a_k^\dagger a_k+\sum_k\omega_k b_k^\dagger b_k+|1\rangle\langle 1|\sum_k g_k\left(a_k^\dagger+a_k\right)+|2\rangle\langle 2|\sum_k g_k\left(b_k^\dagger+b_k\right), \tag{S1}$$

where we have assumed that the dimer is subject to two local harmonic-oscillator baths with the same parameters.

In the experiment, the system is initialized to $|1\rangle$ and followed by a $\pi/2$ pulse, i.e.,

$$|\psi(0)\rangle=\exp\left(i\frac{\pi}{4}\sigma_x\right)|1\rangle=\left(|1\rangle+i|2\rangle\right)/\sqrt{2}. \tag{S2}$$

And the bath is in thermal equilibrium, i.e.,

$$\rho_B=\prod_k^{\otimes}\frac{1}{Z_k}\sum_{n=0}^{\infty}\exp(-n\beta\omega_k)|n\rangle_{a_k}\langle n|\otimes\prod_{k'}^{\otimes}\frac{1}{Z_{k'}}\sum_{m=0}^{\infty}\exp(-m\beta\omega_{k'})|m\rangle_{b_{k'}}\langle m|, \tag{S3}$$

where the partition function of kth bath mode is $Z_k=(1-e^{-\beta\omega_k})^{-1}$. Then, the system evolves under the Hamiltonian (S1) for a time interval t and thus results in

$$\rho(t)=\mathrm{Tr}_B\left[U(t)|\psi(0)\rangle\langle\psi(0)|\otimes\rho_B U^\dagger(t)\right]=\begin{pmatrix}a(t) & b(t)\\ b^*(t) & 1-a(t)\end{pmatrix}. \tag{S4}$$

Finally, after applying a reverse $\pi/2$ pulse, we measure the population of $|1\rangle$ in the final state, i.e.,

$$\rho(t_f)=\exp\left(-i\pi\sigma_x/4\right)\rho(t)\exp\left(i\pi\sigma_x/4\right)=\frac{1}{2}\begin{pmatrix}1+i(b-b^*) & (b+b^*)-i(1-2a)\\ (b+b^*)+i(1-2a) & 1-i(b-b^*)\end{pmatrix}. \tag{S5}$$

Thus, the populations of $|1\rangle$ reads

$$P_1(t_f)=\frac{1}{2}\left[1+i(b-b^*)\right]. \tag{S6}$$

The off-diagonal element can be calculated as

$$b(t)=\mathrm{Tr}_B\left[U(t)|1\rangle\langle 2|\otimes\rho_B U^\dagger(t)\right]=\exp[-i(\varepsilon_D-\varepsilon_A)t]\prod_{k,k'}I_k^{(a)}I_{k'}^{(b)}, \tag{S7}$$

where

$$H_1=\varepsilon_D+\sum_k\omega_k a_k^\dagger a_k+\sum_k\omega_k b_k^\dagger b_k+\sum_k g_k\left(a_k^\dagger+a_k\right), \tag{S8}$$

$$H_2=\varepsilon_A+\sum_k\omega_k a_k^\dagger a_k+\sum_k\omega_k b_k^\dagger b_k+\sum_k g_k\left(b_k^\dagger+b_k\right), \tag{S9}$$

$$I_k^{(a)}=\left[I_k^{(b)}\right]^*=\mathrm{Tr}_B\left[\exp\left(-i\left[\omega_k a_k^\dagger a_k+g_k\left(a_k^\dagger+a_k\right)\right]t\right)\frac{1}{Z_k}\sum_{n=0}^{\infty}\exp(-n\beta\omega_k)|n\rangle_{a_k}\langle n|\exp\left(i\omega_k t a_k^\dagger a_k\right)\right]. \tag{S10}$$

Hereafter, we shall explicitly give the expression of $I_k^{(a)}$ as

$$I_k^{(a)}=\frac{1}{Z_k}\mathrm{Tr}_B\left[D_k^\dagger\left(\frac{g_k}{\omega_k}\right)\exp\left(-i\omega_k t a_k^\dagger a_k\right)\exp\left(i\frac{g_k^2}{\omega_k}t\right)D_k\left(\frac{g_k}{\omega_k}\right)\exp\left(-\beta\omega_k a_k^\dagger a_k\right)\exp\left(i\omega_k t a_k^\dagger a_k\right)\right], \tag{S11}$$

where the displacement operator is $D_k(\alpha)=\exp\left[\alpha\left(a_k^\dagger-a_k\right)\right]$. By using the identity

$$\exp\left(i\omega_k t a_k^\dagger a_k\right)a_k\exp\left(-i\omega_k t a_k^\dagger a_k\right)=a_k\exp(-i\omega_k t), \tag{S12}$$

$I_k^{(a)}$ is simplified as

$$I_k^{(a)} = \frac{1}{Z_k} \exp\left(i\frac{g_k^2}{\omega_k} t - \frac{ig_k^2}{\omega_k^2} \sin\omega_k t \right) \mathrm{Tr}_B \left[\exp\left\{ \frac{g_k}{\omega_k} \left[a_k^\dagger \left(1 - e^{i\omega_k t}\right) + a_k \left(e^{-i\omega_k t} - 1\right) \right] \right\} \exp\left(-\beta\omega_k a_k^\dagger a_k \right) \right], \tag{S13}$$

where in the last line we have used the Baker-Hausdorff formula [S6] $e^A e^B = e^{[A,B]/2} e^{A+B}$. Then, we apply the identity

$$\mathrm{Tr}_B \left[\exp\left(r_1 a_k + r_2 a_k^\dagger \right) \frac{\exp\left(-\beta\omega_k a_k^\dagger a_k \right)}{Z_k} \right] = \exp\left[\frac{1}{2} r_1 r_2 \coth\left(\frac{\beta\omega_k}{2} \right) \right] \tag{S14}$$

to the above equation, we obtain $I_k^{(a)}$ as

$$I_k^{(a)} = \exp\left\{ -\frac{g_k^2}{\omega_k^2} \left[(1 - \cos\omega_k t) \coth\left(\frac{\beta\omega_k}{2} \right) + i \left(\sin\omega_k t - \omega_k t \right) \right] \right\}. \tag{S15}$$

By inserting $I_k^{(a)}$ into $b(t)$, we have

$$b(t) = \exp\left\{ -i \left(\varepsilon_D - \varepsilon_A \right) t - 2\mathrm{Re}[g(t)] \right\}, \tag{S16}$$

where the lineshape function reads

$$g(t) = \sum_k \frac{g_k^2}{\omega_k^2} \left[(1 - \cos\omega_k t) \coth\left(\frac{\beta\omega_k}{2} \right) + i \left(\sin\omega_k t - \omega_k t \right) \right]. \tag{S17}$$

The population of $|1\rangle$ reads

$$P_1(t_f) = \frac{1}{2} \left\{ 1 + \exp(-2\mathrm{Re}[g(t_f)]) \cos(\varepsilon_D - \varepsilon_A) t_f \right\}. \tag{S18}$$

Since the spectral density is defined as

$$J(\omega) = \sum_k g_k^2 \, \delta(\omega - \omega_k) = \int d\omega_k \, \rho(\omega_k) \, g_k^2 \, \delta(\omega - \omega_k) = \rho(\omega_k) g_k^2 |_{\omega_k = \omega} \tag{S19}$$

with $\rho(\omega_k)$ being density of states of bath, the lineshape function can explicitly given as

$$g(t) = \int_0^{\omega_c} d\omega_k \frac{2\lambda\Lambda}{(\omega_k^2 + \Lambda^2)\,\omega_k} \left[(1 - \cos\omega_k t) \coth\left(\frac{\beta\omega_k}{2} \right) + i \left(\sin\omega_k t - \omega_k t \right) \right], \tag{S20}$$

where we assumed a Drude-Lorentz form spectral density

$$J(\omega) = \frac{2\lambda\Lambda\omega}{\omega^2 + \Lambda^2} \tag{S21}$$

with λ and Λ being the reorganization energy and cutoff frequency respectively.

By using a Matsubara expansion [S18], the lineshape function is explicitly calculated as

$$g(t) = \frac{\lambda}{\Lambda} \left[\cot\left(\frac{\beta\Lambda}{2} - i \right) \right] \left(e^{-\Lambda t} + \Lambda t - 1 \right) + \frac{4\lambda\Lambda}{\beta} \sum_{n=1}^{\infty} \frac{e^{-\nu_n t} + \nu_n t - 1}{\nu_n \left(\nu_n^2 - \Lambda^2 \right)}, \tag{S22}$$

where $\nu_n = 2\pi n/\beta$ and $\beta = 1/(k_B T)$.

In Sec. 3, we will demonstrate that in order to simulate the photosynthetic dynamics in NMR, the following relations should be fulfilled

$$\chi(t) = \mathrm{Re}[g(t)], \tag{S23}$$

$$\omega_L = \varepsilon_D - \varepsilon_A. \tag{S24}$$

2. HIERARCHICAL EQUATIONS OF MOTION (HEOM)

The hierarchical equations of motion (HEOM) formalism has become an important method for studying quantum open systems [S7–S9]. In this section, we describe the application of the HEOM method for studying the excitation energy transfer (EET) in photosynthetic systems [S8, S9].

We discuss the EET dynamics in a photosynthetic complex containing four pigments, and each pigment is modeled by a two-level system. The following Frenkel exciton Hamiltonian [S1, S10], studying EET dynamics, consists of three parts,

$$H_{\text{tot}} = H_{\text{el}} + H_{\text{ph}} + H_{\text{el-ph}}, \tag{S25}$$

where

$$H_{\text{el}} = \sum_{j=1}^{4} \varepsilon_j |j\rangle\langle j| + \sum_{j<k}^{4} J_{jk} \left(|j\rangle\langle k| + |k\rangle\langle j| \right), \tag{S26}$$

$$H_{\text{ph}} = \sum_{j=1}^{4} H_{\text{ph},j} = \sum_{j=1}^{4} \sum_{m} \omega_{jm} \left(p_{jm}^2 + q_{jm}^2 \right)/2, \tag{S27}$$

$$H_{\text{el-ph}} = \sum_{j=1}^{4} H_{\text{el-ph},j} = \sum_{j=1}^{4} V_j \mu_j. \tag{S28}$$

In the above, $|j\rangle$ represents the state where only the jth pigment is in its electronic excited state and all others are in their electronic ground state. Moreover, this

$$\varepsilon_j = \varepsilon_j^0 + \lambda_j \tag{S29}$$

is the so-called site energy of the jth pigment, where ε_j^0 is the excited electronic energy of the jth pigment in the absence of phonons and λ_j is the reorganization energy of the jth pigment. Furthermore, J_{jk} is the electronic coupling between pigments i and j. Also, ω_m, p_{jm} and q_{jm} are the frequency, dimensionless coordinate, and conjugate momentum of the mth phonon mode, respectively. Here,

$$V_j = |j\rangle\langle j|, \tag{S30}$$

$$\mu_j = -\sum_{m} c_{jm} q_{jm} \tag{S31}$$

with c_{jm} being the coupling constant between the jth pigment and mth phonon mode. For simplicity, we assume that the phonon modes associated with different pigments are uncorrelated.

The reduced density operator of the system

$$\rho(t) = \text{Tr}_{\text{ph}} \left\{ \rho_{\text{tot}}(t) \right\} \tag{S32}$$

with ρ_{tot} being the density operator for the total system can adequately describe the EET dynamics. At the initial time $t = 0$, we assume that the total system is in the factorized product state of the form

$$\rho_{\text{tot}}(0) = \rho(0) \frac{\exp\left(-\beta H_{\text{ph}}\right)}{\text{Tr}\exp\left(-\beta H_{\text{ph}}\right)}. \tag{S33}$$

In accordance to the vertical Franck-Condon transition [S8, S9], the initial condition (S33) is appropriate in electronic excitation processes. In this work, we adopt the spectral density of the overdamped Brownian oscillator model, $J_j(\omega) = \frac{2\lambda_j \gamma_j \omega}{\omega^2 + \gamma_j^2}$, to describe the coupling between the jth pigment and the environmental phonons. For this modeling, the timescale of the phonon relaxation is simply, $\tau_c = \gamma_j^{-1}$. According to the reorganization dynamics, one can determine the reorganization energy λ_j.

For high temperatures $\beta\gamma_j < 1$, the following hierarchically coupled equations of motion for the reduced density operator with the overdamped Brownian oscillator model is given by

$$\frac{\partial}{\partial t}\sigma(\mathbf{n}, t) = -\left(i\ell_e + \sum_{j=1}^{4} n_j \gamma_j \right) \sigma(\mathbf{n}, t) + \sum_{j=1}^{4} \left[\Phi_j \sigma(\mathbf{n}_{j+}, t) + n_j \Theta_j \sigma(\mathbf{n}_{j-}, t) \right], \tag{S34}$$

where $\mathbf{n} = (n_1, n_2, n_3, n_4)$, $\mathbf{n}_{j\pm} = (n_1, \cdots, n_j \pm 1, \cdots, n_4)$ are three sets of nonnegative integers. The phonon-induced relaxation operators are written by

$$\Phi_j = i V_j^{\times}, \tag{S35}$$

$$\Theta_j = i \left(2\lambda_j T V_j^{\times} - i\lambda_j \gamma_j V_j^{o} \right), \tag{S36}$$

where $O^{\times}f=[O,f]=Of-fO$, $O^{o}f=\{O,f\}=Of+fO$ are the hyper-operator notations. In addition, $\rho(t)=\sigma(\mathbf{0},t)$, and the other $\sigma(\mathbf{n}\neq\mathbf{0},t)$ are auxiliary operators considering the fluctuation and dissipation. The Liouvillian operator ℓ_e corresponds to the electronic Hamiltonian H_e.

We terminate Eq. (S34), when the integers n_j's satisfy

$$N=\sum_{j=1}^{4}n_j\gg\frac{\omega_e}{\min\left(\gamma_1,\gamma_2,\gamma_3,\gamma_4\right)}, \tag{S37}$$

where ω_e is a characteristic frequency of the system dynamics ℓ_e [S8]. The required number of auxiliary density operators $\sigma(\mathbf{n},t)$ is given by

$$\sum_{k=0}^{N}\left(\begin{array}{c}k+4-1\\4-1\end{array}\right)=\frac{(4+N)!}{4!N!}. \tag{S38}$$

3. DYNAMICS WITH CLASSICAL PURE-DEPHASING NOISE

i. General Case

In this section, inspired by Ref. [S3], we provide a detailed calculation for the dynamics in the classical pure-dephasing noise. The total Hamiltonian

$$H\left(t\right)=H_0\left(t\right)+H_c\left(t\right) \tag{S39}$$

is divided into two parts, i.e. the control Hamiltonian $H_c\left(t\right)=\vec{h}\left(t\right)\cdot\vec{\sigma}$, and the noise Hamiltonian $H_0\left(t\right)=\vec{\beta}\left(t\right)\cdot\vec{\sigma}$, where $\vec{h}\left(t\right)=\left(h_x\left(t\right),h_y\left(t\right),h_z\left(t\right)\right)$, $\vec{\beta}\left(t\right)=\left(\beta_x\left(t\right),\beta_y\left(t\right),\beta_z\left(t\right)\right)$, $\vec{\sigma}=\left(\sigma_x,\sigma_y,\sigma_z\right)$.

In the rotating frame with respect to $U_c\left(t\right)=\mathcal{T}\exp\left[-i\int_0^t d\tau H_c\left(\tau\right)\right]$, the noise Hamiltonian reads

$$\widetilde{H}_0\left(t\right)=U_c^{\dagger}\left(t\right)H_0\left(t\right)U_c\left(t\right). \tag{S40}$$

And the propagator in this frame is correspondingly

$$\widetilde{U}\left(t\right)=\mathcal{T}\exp\left[-i\int_0^t d\tau\widetilde{H}_0\left(\tau\right)\right]. \tag{S41}$$

Therefore, transformed back to the Schrödinger picture, the propagator is written as

$$U\left(t\right)=U_c\left(t\right)\widetilde{U}\left(t\right). \tag{S42}$$

Let us now consider

$$\widetilde{H}_0\left(t\right)=U_c^{\dagger}\left(t\right)\vec{\beta}\left(t\right)\cdot\vec{\sigma}U_c\left(t\right)=\sum_{i,j}\beta_i\left(t\right)R_{ij}\left(t\right)\sigma_j, \tag{S43}$$

where

$$R_{ij}\left(t\right)=\frac{1}{2}\mathrm{Tr}\left[U_c^{\dagger}\left(t\right)\sigma_iU_c\left(t\right)\sigma_j\right], \tag{S44}$$

and in the last line of Eq. (S43) we have used the relation $\mathrm{Tr}\left[\sigma_i\sigma_j\right]=2\delta_{ij}$. Hereafter, we shall use the compact definition

$$\overrightarrow{R}=\left(R_x\left(t\right),R_y\left(t\right),R_z\left(t\right)\right)^T, \tag{S45}$$

where

$$R_i\left(t\right)=\left(R_{ix}\left(t\right),R_{iy}\left(t\right),R_{iz}\left(t\right)\right). \tag{S46}$$

When

$$\widetilde{U}\left(t\right)=\exp\left[-i\sum_{\mu=1}^{\infty}\Phi_{\mu}\left(\tau\right)\right], \tag{S47}$$

according to the Magnus expansion [S15], we have

$$\Phi_1(\tau) = \int_0^\tau dt \widetilde{H}_0(t), \tag{S48}$$

$$\Phi_2(\tau) = -\frac{i}{2}\int_0^\tau dt_1 \int_0^{t_1} dt_2 \left[\widetilde{H}_0(t_1), \widetilde{H}_0(t_2)\right], \tag{S49}$$

$$\Phi_3(\tau) = -\frac{1}{6}\int_0^\tau dt_1 \int_0^{t_1} dt_2 \int_0^{t_2} dt_3 \left\{\left[\widetilde{H}_0(t_1), \left[\widetilde{H}_0(t_2), \widetilde{H}_0(t_3)\right]\right] + \left[\widetilde{H}_0(t_3), \left[\widetilde{H}_0(t_2), \widetilde{H}_0(t_1)\right]\right]\right\}. \tag{S50}$$

By using the identity $[\overrightarrow{u}\vec{\sigma}, \overrightarrow{v}\vec{\sigma}] = 2i\left(\overrightarrow{u} \times \overrightarrow{v}\right)\vec{\sigma}$, the propagator (S47) can be rewritten as

$$\widetilde{U}(t) = \exp\left[-i\sum_\mu \vec{a}_\mu(\tau)\cdot\vec{\sigma}\right], \tag{S51}$$

where

$$\vec{a}_1(\tau) = \sum_i \int_0^\tau dt\ \beta_i R_i(t), \tag{S52}$$

$$\vec{a}_2(\tau) = \sum_{i,j} \int_0^\tau dt_1 \int_0^{t_1} dt_2\ \beta_i(t_1)\ \beta_j(t_1)\ \widetilde{R}_{ij}(t_1,t_2), \tag{S53}$$

$$\vec{a}_3(\tau) = \frac{2}{3}\sum_{i,j,k} \int_0^\tau dt_1 \int_0^{t_1} dt_2 \int_0^{t_2} dt_3\ \beta_i(t_1)\ \beta_j(t_2)\ \beta_k(t_3)\ \widetilde{R}_{ijk}(t_1,t_2,t_3), \tag{S54}$$

with

$$\widetilde{R}_{ij}(t_1,t_2) = R_i(t_1)\times R_j(t_2), \tag{S55}$$

$$\widetilde{R}_{ijk}(t_1,t_2,t_3) = R_i(t_1)\times\left[R_j(t_2)\times R_k(t_3)\right] + R_k(t_3)\times\left[R_j(t_2)\times R_i(t_1)\right]. \tag{S56}$$

To calculate the fidelity of the operation described by

$$U_c(t) = \mathcal{T}\exp\left[-i\int_0^t d\tau H_c(\tau)\right], \tag{S57}$$

we use the Hilbert-Schmidt inner product to measure the fidelity as

$$\mathcal{F}(\tau) = \frac{1}{4}\left|\mathrm{Tr}\left[U_c^\dagger(\tau)U_c(\tau)\widetilde{U}(\tau)\right]\right|^2 = \frac{1}{2}\left[1+\sum_{n=0}^{\infty}(-1)^m\frac{2^{2m}}{(2m)!}\langle a^{2m}\rangle\right], \tag{S58}$$

where a is the modulus of the vector $\vec{a}(\tau)$, and $\langle\cdots\rangle$ is averaged over all possible noise trajectories. In the above equation, the lowest order term is

$$\langle a^2\rangle = \langle aa^T\rangle = \langle a_1a_1^T\rangle + \langle a_2a_2^T\rangle + \cdots + 2\left(\langle a_1a_2^T\rangle + \langle a_1a_3^T\rangle + \langle a_1a_4^T\rangle + \cdots\right). \tag{S59}$$

Thus, the fidelity can be expanded as

$$\mathcal{F}(\tau) \simeq 1 - \langle a_1a_1^T\rangle = 1 - \sum_{i,j,k}\int_0^\tau dt_1\int_0^\tau dt_2\ \langle\beta_i(t_1)\beta_j(t_2)\rangle R_{ik}(t_1)R_{jk}^*(t_2), \tag{S60}$$

where we have used the relation $R_{kj}^T(\tau) = R_{jk}^*(\tau)$.

By introducing the Fourier transform of the cross-power spectrum

$$\langle\beta_i(t_1)\beta_j(t_2)\rangle = \frac{1}{2\pi}\int_{-\infty}^{\infty} d\omega\ S_{ij}(\omega)e^{i\omega(t_2-t_1)}, \tag{S61}$$

we have

$$\begin{aligned}\mathcal{F}(\tau) &= 1 - \frac{1}{2\pi}\sum_{i,j,k}\int_0^\tau dt_1\int_0^\tau dt_2\int_{-\infty}^{\infty} d\omega\ S_{ij}(\omega)e^{i\omega(t_2-t_1)}R_{ik}(t_1)R_{jk}^*(t_2)\\ &= 1 - \frac{1}{2\pi}\sum_{i,j,k}\int_{-\infty}^{\infty}\frac{d\omega}{\omega^2}S_{ij}(\omega)\left(-i\omega\right)\int_0^\tau dt_1\ R_{ik}(t_1)e^{-i\omega t_1}\left(i\omega\right)\int_0^\tau dt_2\ R_{jk}^*(t_2)e^{i\omega t_2}\\ &= 1 - \frac{1}{2\pi}\sum_{i,j,k}\frac{d\omega}{\omega^2}S_{ij}(\omega)R_{ik}(\omega)R_{jk}^*(\omega),\end{aligned} \tag{S62}$$

where we have defined

$$R_{ik}(\omega) = -i\omega \int_0^\tau dt\ R_{ik}(t) e^{-i\omega t}. \tag{S63}$$

ii. Ramsey Fringes

In the following, we shall consider a special case where $[H_0(t), H_c(t)] = 0$. At the end of this subsection, we will provide the deviation for Ramsey-interferometer experiment. In this case, we assume the total Hamiltonian as

$$H(t) = \frac{\omega_L}{2}\sigma_z + \beta_z(t)\sigma_z. \tag{S64}$$

Thus, the control Hamiltonian is $H_c = \frac{\omega_L}{2}\sigma_z$, and the noise Hamiltonian is $H_0(t) = \beta_z(t)\sigma_z$.

In the rotating frame with respect to $U_c(t) = \exp\left(-i\frac{\omega_L t}{2}\sigma_z\right)$, the noise Hamiltonian reads

$$\widetilde{H}_0(t) = U_c^\dagger(t) H_0(t) U_c(t) = H_0(t), \tag{S65}$$

because $[H_c, H_0(t)] = 0$.

And the propagator in this frame is correspondingly

$$\widetilde{U} = \exp\left[-i\int_0^t d\tau\ \beta_z(\tau)\sigma_z\right]. \tag{S66}$$

Therefore, transformed back to the Schrödinger picture, the propagator is written as

$$U(t) = U_c(t)\widetilde{U}(t) = \exp\left(-i\frac{\omega_L t}{2}\sigma_z\right)\exp\left[-i\int_0^t d\tau\ \beta_z(\tau)\sigma_z\right]. \tag{S67}$$

In the experiment, the system is initialized to $|0\rangle$ and followed by a $\pi/2$ pulse, i.e.

$$|\psi(0)\rangle = \exp\left(i\frac{\pi}{4}\sigma_x\right)|0\rangle = \left(|0\rangle + i|1\rangle\right)/\sqrt{2}. \tag{S68}$$

Then, the system evolves under the Hamiltonian (S64) for a time interval t and thus results in

$$|\psi(t)\rangle = \frac{1}{\sqrt{2}}U(t)\left(|0\rangle + i|1\rangle\right) = \frac{1}{\sqrt{2}}\left(e^{-i\phi(t)}|0\rangle + ie^{i\phi(t)}|1\rangle\right), \tag{S69}$$

where

$$\phi(t) = \phi_A(t) + \phi_B(t), \tag{S70}$$

$$\phi_A(t) = \frac{\omega_L t}{2}, \tag{S71}$$

$$\phi_B(t) = \int_0^t d\tau\ \beta_z(\tau). \tag{S72}$$

Finally, after applying a reverse $\pi/2$ pulse, we measure the population of $|0\rangle$ in the final state, i.e.

$$|\psi_f(t)\rangle = \frac{1}{\sqrt{2}}e^{-i\pi\sigma_z/4}\left(e^{-i\phi(t)}|0\rangle + ie^{i\phi(t)}|1\rangle\right) = \cos\phi(t)|0\rangle + \sin\phi(t)|1\rangle. \tag{S73}$$

Thus, the population of $|0\rangle$ reads

$$P_0(t) = \cos^2\phi(t) = \frac{1}{2}\left[1 + \cos 2\phi_A\langle\cos 2\phi_B(t)\rangle - \sin 2\phi_A(t)\langle\sin 2\phi_B(t)\rangle\right], \tag{S74}$$

where $\langle\cdots\rangle$ is averaged over all possible random realizations. If we further assume a Gaussian noise, $\langle\phi_B^{2n-1}(t)\rangle = 0$ for any positive integer n, $P_0(t)$ can be simplified as

$$P_0(t) = \frac{1}{2}\left[1 + \cos 2\phi_A(t)\langle\cos 2\phi_B(t)\rangle\right] = \frac{1}{2}\left[1 + \cos 2\phi_A(t)\sum_{n=0}^{\infty}(-1)^n\frac{2^{2n}}{(2n)!}\langle\phi_B^{2n}(t)\rangle\right]. \tag{S75}$$

For the lowest nontrivial order $n = 1$, we have

$$\chi(t) = \langle \phi_B^2(t) \rangle = \int_0^t d\tau_1 \int_0^t d\tau_2 \, \langle \beta_z(\tau_1)\beta_z(\tau_2) \rangle = \frac{4}{2\pi} \int_{-\infty}^{\infty} \frac{d\omega}{\omega^2} S_{zz}(\omega) \sin^2 \frac{\omega t}{2}, \tag{S76}$$

where we have introduced the Fourier transform of $\langle \beta_z(\tau_1)\beta_z(\tau_2) \rangle$ as

$$S_{zz}(\omega) = \int_{-\infty}^{\infty} dt \, \langle \beta_z(0)\beta_z(t) \rangle e^{i\omega t} \tag{S77}$$

with $\langle \beta_z(\tau_1)\beta_z(\tau_2) \rangle$ being only dependent on the time interval $\tau_2 - \tau_1$.

For the order with $n = 2$, we have

$$\begin{aligned}
\langle \phi_B^4(t) \rangle &= \int_0^t d\tau_1 \int_0^t d\tau_2 \int_0^t d\tau_3 \int_0^t d\tau_4 \, \langle \beta_z(\tau_1)\beta_z(\tau_2)\beta_z(\tau_3)\beta_z(\tau_4) \rangle \\
&= \int_0^t d\tau_1 \int_0^t d\tau_2 \int_0^t d\tau_3 \int_0^t d\tau_4 \, [\langle \beta_z(\tau_1)\beta_z(\tau_2) \rangle \langle \beta_z(\tau_3)\beta_z(\tau_4) \rangle + \langle \beta_z(\tau_1)\beta_z(\tau_3) \rangle \langle \beta_z(\tau_2)\beta_z(\tau_4) \rangle \\
&\quad + \langle \beta_z(\tau_1)\beta_z(\tau_4) \rangle \langle \beta_z(\tau_2)\beta_z(\tau_3) \rangle] \\
&= 3 \int_0^t d\tau_1 \int_0^t d\tau_2 \int_0^t d\tau_3 \int_0^t d\tau_4 \, \langle \beta_z(\tau_1)\beta_z(\tau_2) \rangle \langle \beta_z(\tau_3)\beta_z(\tau_4) \rangle = 3\chi^2(t).
\end{aligned} \tag{S78}$$

For the order with arbitrary integer n, we have

$$\begin{aligned}
\langle \phi_B^{2n}(t) \rangle &= \int_0^t d\tau_1 \int_0^t d\tau_2 \cdots \int_0^t d\tau_{2n} \, \langle \beta_z(\tau_1)\beta_z(\tau_2) \cdots \beta_z(\tau_{2n}) \rangle \\
&= \int_0^t d\tau_1 \int_0^t d\tau_2 \int_0^t d\tau_3 \int_0^t d\tau_4 \, [\langle \beta_z(\tau_1)\beta_z(\tau_2) \rangle \langle \beta_z(\tau_3)\beta_z(\tau_4) \rangle \cdots \langle \beta_z(\tau_{2n-1})\beta_z(\tau_{2n}) \rangle + \cdots] \\
&= \frac{(2n)!}{2^n n!} \left[\frac{4}{2\pi} \int_{-\infty}^{\infty} \frac{d\omega}{\omega^2} S_{zz}(\omega) \sin^2 \frac{\omega t}{2} \right]^n = \frac{(2n)!}{2^n n!} \chi^n(t),
\end{aligned} \tag{S79}$$

where there are $(2n)!/(2^n n!)$ terms in the second line according to Isserlis' theorem if it is a Gaussian noise [S16]. To conclude,

$$P_0(t) = \frac{1}{2} \left[1 + \cos 2\Phi_A(t) \sum_{n=0}^{\infty} (-1)^n \frac{2^{2n}}{(2n)!} \frac{(2n)!}{2^n n!} \chi^n(t) \right] = \frac{1}{2} \left[1 + \cos 2\phi_A(t) e^{-2\chi(t)} \right]. \tag{S80}$$

This predicts that before decaying to the steady value $1/2$ in the long run, $P_0(t)$ will experience oscillations with frequency ω_L.

We assume that

$$\beta_z = \alpha \sum_{j=1}^{J} F(\omega_j)\omega_j \cos(\omega_j t + \psi_j), \tag{S81}$$

where the ψ_j's are random numbers. According to Ref. [S16], the ensemble average is equivalent to the time average for a wide-sense-stationary random process. In this case, the two-time correlation function reads

$$\langle \beta_z(t+\tau)\beta_z(t) \rangle = \lim_{T\to\infty} \frac{1}{2T} \int_{-T}^{T} dt \beta_z(t+\tau)\beta_z(t) = \left(\frac{\alpha}{2} \right)^2 \sum_{j=1}^{J} [\omega_j F(\omega_j)]^2 \left(e^{i\omega_j \tau} + e^{-i\omega_j \tau} \right), \tag{S82}$$

which does not depend on t but τ.

The power spectral density is the Fourier transform of the correlation function, i.e.

$$S_{zz}(\omega) = \int_{-\infty}^{\infty} d\tau \, e^{-i\omega\tau} \langle \beta_z(t+\tau) \beta_z(t) \rangle = \left(\frac{\alpha}{2} \right)^2 \sum_{j=1}^{J} [\omega_j F(\omega_j)]^2 [\delta(\omega - \omega_j) + \delta(\omega + \omega_j)], \tag{S83}$$

where $\delta(\omega \pm \omega_j) = \int_{\infty}^{\infty} dt \, e^{i(\omega \pm \omega_j)t}$. The power spectral density is a set of equally-spaced peaks with distance ω_0 and height $\left(\frac{\alpha}{2} \right)^2 [\omega_j F(\omega_j)]^2$.

If we set $F(\omega_j) = (\omega_j \left(\omega_j^2 + \gamma^2 \right))^{-1/2}$, we have

$$S_{zz}(\omega) = \frac{\alpha^2}{4} \sum_{j=1}^{J} \frac{\omega_j}{\omega_j^2 + \gamma^2} [\delta(\omega - \omega_j) + \delta(\omega + \omega_j)] \tag{S84}$$

and thus $S_{zz}(\omega)$ is the Drude-Lorentz spectral density of the step-function form with cutoff frequency ω_J.

The transverse relaxation time T_2 is defined by

$$2\chi(T_2) = 1. \tag{S85}$$

For photosynthesis, the decoherence is determined by the real part of the lineshape function

$$g(t) = \frac{\lambda}{\Lambda}\left[\cot\left(\frac{\beta\Lambda}{2}\right) - i\right]\exp\left(-\Lambda t + \Lambda t - 1\right) + \frac{4\lambda\Lambda}{\beta}\sum_{n=1}^{\infty}\frac{e^{-\nu_n t + \nu_n t - 1}}{\nu_n\left(\nu_n^2 - \Lambda^2\right)}, \tag{S86}$$

with spectral density $J(\omega) = \frac{2\lambda\Lambda\omega}{\omega^2+\Lambda^2}$, where $\nu_n = 2\pi n/\beta$.

Therefore, in order to simulate photosynthetic dynamics in NMR, we should relate the following two quantities

$$\chi(t) = \mathrm{Re}[g(t)] \tag{S87}$$

and cutoff frequencies in two spectra are equal, i.e.

$$\gamma = \Lambda. \tag{S88}$$

4. ARTIFICIALLY INJECTING NOISE

Here we introduce a method of artificially injecting noises in NMR and ion trap systems, including dephasing noise and amplitude noise [S4, S5].

i. Dephasing Noise

Dephasing noise comes from the inhomogeneous and non-static magnetic field in NMR systems. The corresponding Hamiltonian can be written as $\beta_z(t)\sigma_z$ with

$$\beta_z(t) = \sum_{j=1}^{N}\alpha_z F(\omega_j)\omega_j\cos(\omega_j t + \phi_j), \tag{S89}$$

where $\alpha_i (i = x, y, z)$ is the noise amplitude and ϕ_j is a random phase. $N\omega_0$ determines the high frequency cutoff and ω_0 is the base frequency with $\omega_j = j\omega_0$. The types of noise rely on the function $F(\omega_j)$. The two-time correlation function for $\beta_z(t)$ is then written as

$$\langle\beta_z(t+\tau)\beta_z(t)\rangle = \lim_{T\to\infty}\frac{1}{2T}\int_{-T}^{T}dt\ \beta_z(t+\tau)\beta_z(t) = \left(\frac{\alpha_z}{2}\right)^2\sum_j[\omega_j F(\omega_j)]^2(e^{i\omega_j\tau} + e^{-i\omega_j\tau}), \tag{S90}$$

which does not depend on t but on τ. Applying the Wiener-Khintchine theorem [S17], we then obtain the power spectral density which can describe the energy distribution of the stochastic signal in the frequency domain by Fourier transform

$$S_z(\omega) = \int_{-\infty}^{\infty}d\tau\ e^{-i\omega\tau}\langle\beta_z(t+\tau)\beta_z(t)\rangle = \frac{\pi\alpha_z^2}{2}\sum_{j=1}^{N}[F(\omega_j)\omega_j]^2[\delta(\omega-\omega_j) + \delta(\omega+\omega_j)]. \tag{S91}$$

Hence, we can use the model of power spectral density to reverse the noise distribution in the time domain. For instance, if we want to simulate the power spectral density for $S(\omega) \sim \omega^p$, then the modulation function $F(\omega_j) = (\omega_j)^{p/2-1}$. Taking Eq. (S87) into above,

$$\chi(t) = \alpha_z^2\sum_{j=1}^{N}[F(\omega_j)]^2\sin^2\frac{\omega_j t}{2} \tag{S92}$$

The initial state $|\psi(0)\rangle = \alpha|0\rangle + \beta|1\rangle$ with the dephasing noise of the Hamiltonian $\beta_z(t)\sigma_z$ in the rotating frame after time τ will become

$$|\psi(\tau)\rangle = \exp\left[-i\int_{\tau 1}^{\tau 2}dt\beta_z(t)\sigma_z/2\right](\alpha|0\rangle + \beta|1\rangle) = \exp\left[-i\triangle\theta_\tau\frac{\sigma_z}{2}\right]|\psi(0)\rangle, \tag{S93}$$

where $\triangle\theta_\tau$ is the integral of $\beta_z(t)$. Hence we just rotate the angle $\triangle\theta_\tau$ along the z-axis at the desired point to realize the evolution of the quantum system in the dephasing environment.

ii. Amplitude Noise

Similarly, we can obtain the $\beta_x(t)$ of the amplitude noise as a result of the amplitude fluctuation of the control field,

$$\beta_x(t) = \sum_{j=1}^{N} \alpha_x F(\omega_j) \sin(\omega_j t + \phi_j), \tag{S94}$$

$$F(\omega_j) = (\omega_j)^{p/2}, \tag{S95}$$

and its power spectral density is

$$S(\omega) = \frac{\pi \alpha_x^2}{2} \sum_{j=1}^{N} [F(\omega_j)]^2 [\delta(\omega - \omega_j) + \delta(\omega + \omega_j)] \tag{S96}$$

iii. Parameters for Dephasing Noise of the Drude-Lorentz Form

For the Drude-Lorentz spectrum of the dephasing noise, taking Re$[g(t)]$ equal to $\chi(t)$, we obtain

$$\beta(t) = \sqrt{\frac{2}{\pi}} \sum_{j=1}^{N} F(\omega_j) \omega_j \cos(\omega_j t + \phi_j), \tag{S97}$$

$$F(\omega_j) = \sqrt{\frac{2\lambda\gamma\omega_0 \coth(\frac{\beta\omega_j}{2})}{\omega_j(\omega_j^2 + \gamma^2)}}. \tag{S98}$$

In short, as long as we know the power spectral density of the noise, we can then obtain the time-varying $\beta(t)$ and $\chi(t)$. Table I shows $F(\omega_j)$ for distinct types of dephasing and amplitude noises.

Table I. $F(\omega_j)$ for distinct dephasing and amplitude noises

	Dephasing					Amplitude			
	$1/f^2$	$1/f$	White	Ohmic	Drude-Lorentz	$1/f^2$	$1/f$	White	Ohmic
$F(\omega_j)$	ω_j^{-2}	$\omega_j^{-3/2}$	ω_j^{-1}	$\omega_j^{-1/2}$	$\sqrt{\frac{2\lambda\gamma\omega_0 \coth(\beta\omega_j/2)}{\omega_j(\omega_j^2+\gamma^2)}}$	ω_j^{-1}	$\omega_j^{-1/2}$	ω_j^{0}	$\omega_j^{1/2}$

iv. Parameters for Dephasing Noise of Arbitrary Form

For the general spectrum $J(\omega)$ of the dephasing noise, we make Re$[g(t)]$ and $\chi(t)$ be equal according to Eqs. (S20), (S87), (S92)

$$\alpha_z^2 \sum_{j=1}^{N} [F(\omega_j)]^2 \sin^2 \frac{\omega_j t}{2} = \sum_{j=1}^{N} \frac{J(\omega_j)\omega_0}{\omega_j^2} (1 - \cos\omega_j t) \coth\left(\frac{\beta\omega_j}{2}\right). \tag{S99}$$

After simplifying the above formula, we can obtain

$$F(\omega_j) = \frac{1}{\alpha_z} \sqrt{\frac{2J(\omega_j)\omega_0}{\omega_j^2} \coth\left(\frac{\beta\omega_j}{2}\right)}. \tag{S100}$$

For the B777-complexes in Ref. [S22], of which the spectral density is

$$J(\omega) = \frac{S_0}{s_1 + s_2} \sum_{i=1,2} \frac{s_i}{7!2\Omega_i^4} \omega^3 e^{-(\omega/\Omega_i)^{1/2}} \tag{S101}$$

where $s_1 = 0.8$, $s_2 = 0.5$, $\Omega_1 = 0.069$ meV, $\Omega_2 = 0.24$ meV, $S_0 = 0.5$, the corresponding $F(\omega_j)$ in NMR experiments can be obtained via the above formula (S100).

5. EXPERIMENTAL DETAILS AND RESULTS

Experiments are carried out at room temperature using a Bruker Avance III 400 MHz spectrometer. The sample is chloroform dissolved in d6-acetone as a two-qubit NMR quantum processor where H is the first qubit and C is second qubit. The internal Hamiltonian of the two-qubit system can be described as

$$H_{\text{int}} = \pi\omega_1\sigma_1^z + \pi\omega_2\sigma_2^z + \frac{\pi}{2}J\sigma_1^z\sigma_2^z, \tag{S102}$$

where $\omega_1 = 3206.5$ Hz, $\omega_2 = 7787.9$ Hz are the chemical shifts of the two spins and $J = 215.1$ Hz is the J-coupling strength between two spins. The experimental process is divided into three steps, as shown in Fig. S1.

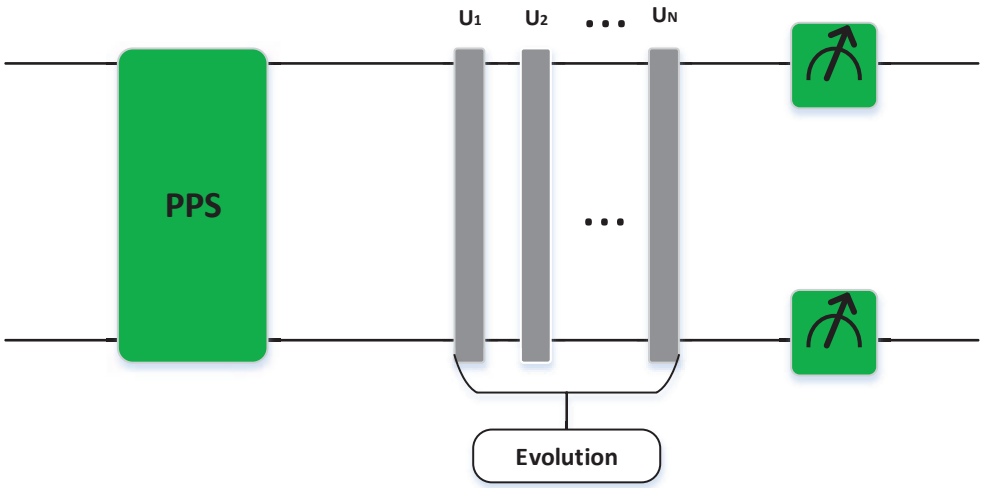

Figure S1. Sequence of the NMR experimental process. It includes three steps: preparation of the pseudo-pure state, Evolution of the Hamiltonian with Drude-Lorentz noise and measuring the probability distribution of four states.

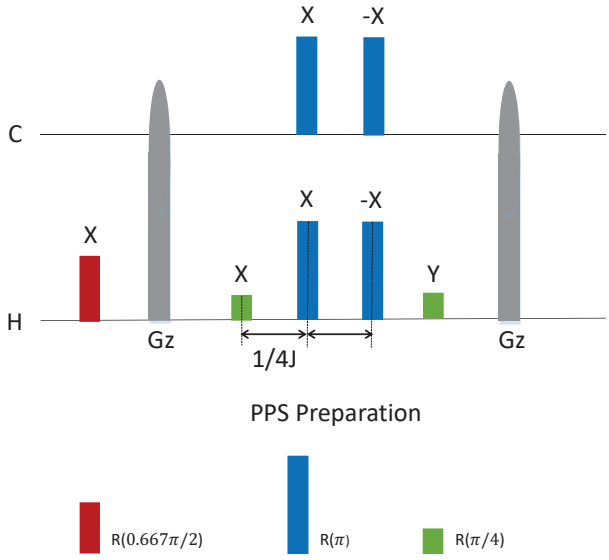

Figure S2. NMR sequences to realize pseudo-pure state. Gz means a z-gradient pulse which is used to cancel the polarization in xy plane.

i. Preparation of the Pseudo-pure State

The thermal equilibrium state for the two qubit system is

$$\rho_{\text{eq}} \approx \frac{1}{4}I + \epsilon(\gamma_H \sigma_1^z + \gamma_C \sigma_2^z), \tag{S103}$$

where I is a 4×4 identity matrix, $\epsilon \approx 10^{-5}$ describes the polarization, and γ_H and γ_C represent the gyromagnetic ratios of the ^{1}H and ^{13}C nuclei, respectively. The spatial average technique [S12] is used to obtain a pseudo-pure state

$$\rho_{00} = \frac{1-\epsilon}{4}I + \epsilon|00\rangle\langle 00| \tag{S104}$$

and the related pulse sequence is depicted in Fig. S2. Thus we only focus on the part $|00\rangle$ as the entire system behaves since the identity part does not influence the unitary operations or measurements in NMR experiments.

ii. Evolution of the Hamiltonian with the Drude-Lorentz Noise

The total Hamiltonian for simulating photosynthetic EET in the NMR system is

$$H(t) = H_S + n_1(t)\sigma_1^z + n_2(t)\sigma_2^z, \tag{S105}$$

$$n_1(t) = \frac{\beta_1(t) + \beta_2(t)}{2}, \tag{S106}$$

$$n_2(t) = \frac{\beta_1(t) - \beta_2(t)}{2}, \tag{S107}$$

where H_S is the system Hamiltonian, and $\beta_i(t)$ $(i = 1, 2)$ are the time-dependent Drude-Lorentz noises. In experiments, the evolution can have L discretized steps, and the evolution time is $t = L\Delta t$ with

$$U(t) = \mathcal{T}\exp\left[\int_0^t -iH(t')dt'\right] = \prod_{i=1}^{L} U_i = \prod_{i=1}^{L}\exp[-iH_i\Delta t], \tag{S108}$$

where H_i is the time-independent Hamiltonian at point $t_i = i\Delta t$. Note $U(t)$ is calculated by the gradient ascent pulse engineering (GRAPE) method with 5 ms of each pulse to reduce the accumulated pulse errors in experiments.

iii. Measure the Probability Distribution of Four States

Our goal now is to acquire probability distributions of four states $|00\rangle$, $|01\rangle$, $|10\rangle$, $|11\rangle$; namely, the four diagonal values of the final density matrix. The density matrices of the output states are reconstructed completely via quantum state tomography (QST) [S13]. In the QST theory, the density matrix of the system can be estimated from ensemble averages of a set of observables. For the one-qubit system, the observable set is $\{\sigma_i\}$ $(i = 0, 1, 2, 3)$, where $\sigma_0 = I$ is the identity, $\sigma_1 = X$, $\sigma_2 = Y$, $\sigma_3 = Z$ are the Pauli matrices. The NMR signal is

$$S(t) \propto [\langle X\rangle + i\langle Y\rangle]e^{i\omega t}, \tag{S109}$$

which is oscillating at the frequency ω and $\langle X\rangle$ and $\langle Y\rangle$ are obtained in practice by Fourier transforming $S(t)$ and integrating the real and imaginary spectra, respectively. The signal becomes

$$S^Y(t) \propto [-\langle Z\rangle + i\langle Y\rangle]e^{i\omega t} \tag{S110}$$

after applying $\exp[-i\pi Y/4]$. The density operator of one-qubit can be estimated by

$$\rho = \frac{1}{2}I + \langle X\rangle\, X + \langle Y\rangle Y + \langle Z\rangle\, Z. \tag{S111}$$

For the two-qubit system, the observable set is $\{\sigma_i \otimes \sigma_j\}(i, j = 0, 1, 2, 3)$. In our experiments, the complete density matrix tomography is not necessary. All we need is to perform two experiments in which the reading-out pulses $\exp(-i\pi Y/4) \otimes I$ and $I \otimes \exp(-i\pi Y/4)$ are respectively implemented on the final states of ^{1}H and ^{13}C and the corresponding qubits that need to be

observed are respectively ^{1}H and ^{13}C. Then the probability distribution of four states are obtained by the results of measuring $\langle ZI\rangle$, $\langle IZ\rangle$, $\langle ZZ\rangle$. Then the probability distribution of four states are respectively

$$\rho_{00} = \frac{1}{4}I + \langle ZI\rangle + \langle IZ\rangle + \langle ZZ\rangle, \tag{S112}$$

$$\rho_{01} = \frac{1}{4}I + \langle ZI\rangle - \langle IZ\rangle - \langle ZZ\rangle, \tag{S113}$$

$$\rho_{10} = \frac{1}{4}I - \langle ZI\rangle + \langle IZ\rangle - \langle ZZ\rangle, \tag{S114}$$

$$\rho_{11} = \frac{1}{4}I - \langle ZI\rangle - \langle IZ\rangle - \langle ZZ\rangle. \tag{S115}$$

6. GRADIENT ASCENT PULSE ENGINEERING (GRAPE) ALGORITHM

Here we describe the GRAPE technique proposed by Glaser *et al.* [S14] which has been frequently used in NMR experiments. For an n-qubit NMR system, the total Hamiltonian contains the internal term

$$H_t = H_{\text{int}} + H_{\text{RF}}, \tag{S116}$$

and the radio frequency (RF) term

$$H_{\text{RF}} = -\sum_{k=1}^{n} \gamma_k B_k \left[\cos(\omega_{\text{RF}}^k t + \phi_k)\sigma_x^k + \sin(\omega_{\text{RF}}^k t + \phi_k)\sigma_y^k\right], \tag{S117}$$

where B_k and ϕ_k are the amplitude and phase of the control field on the kth nuclear spin. The goal of the GRAPE technique is to find the optimal parameters B_k and ϕ_k of the RF field by iteration to control the designed evolution U_T very close to desired target evolution U_D. Assuming that the total time of RF field is T, which is divided into L discrete segments. The time of each segment is $\Delta t = T/L$ and the time propagator of the jth segment can be expressed as

$$U_j = \exp[-i\Delta t(H_{\text{int}} + \sum_k u_x^k(j)\sigma_x^k + \sum_k u_x^k(j)\sigma_x^k)]. \tag{S118}$$

Thus, the total evolution is $U_T = U_N U_{N-1}\cdots U_2 U_1$. The fidelity to the target evolution U_T can be expressed as $\mathcal{F} = |\text{Tr}(U_D^\dagger U_T)|/2^n$, which is also called the fitness function. The GRAPE algorithm considers the fidelity $\mathcal{F}$ as the extreme value optimization of the multi-function. We calculate the gradient function to first order,

$$g_{x,y}^k(j) = \frac{\partial F}{\partial u_{x,y}^k(j)} \approx -\frac{2}{2^n}\text{Re}[U_D^\dagger U_N \cdots (-i\Delta t\sigma_{x,y}^k)U_m \cdots U_1]. \tag{S119}$$

The fitness functions can be increased in the gradient iteration,

$$u_{x,y}^k(j) \to u_{x,y}^k(j) + \varepsilon \cdot g_{x,y}^k(j), \tag{S120}$$

where ε is a suitable and small step size. The GRAPE procedure starts from an initial guess input and evaluates the corresponding gradients $g_{x,y}^k(j)$ and then keeps iterating until the fitness function reaches the desired value.

7. RESULTS OF THE NUMERICAL SIMULATIONS

Before the experimental demonstration, we shall numerically demonstrate that the photosynthetic light harvesting can be exactly mimicked by the NMR quantum simulation using the GRAPE algorithm.

In our numerical simulations, we used the following parameters, i.e., $\gamma_{\text{NMR}} = 2\pi \times 45$ kHz, $\lambda_{\text{NMR}} = 2\pi \times 0.01$ kHz, $T_{\text{EET}} = 3 \times 10^4$ K, and $T_{\text{NMR}} = 5 \times 10^{-5}$ K. Also, $\hbar = 1.055 \times 10^{-34}$ J $\cdot$ s, and $k_B = 1.381 \times 10^{-23}$ J/K. The Hamiltonian for four-pigments in the single-excitation subspace is

$$H_{\text{NMR}} = 2\pi \times \begin{pmatrix} 650 & 6.3040 & 0.8059 & 0.2370 \\ 6.3040 & 645 & 6.5950 & 0.8059 \\ 0.8059 & 6.5950 & 615 & 6.3040 \\ 0.2370 & 0.8059 & 6.3040 & 610 \end{pmatrix} \text{kHz}. \tag{S121}$$

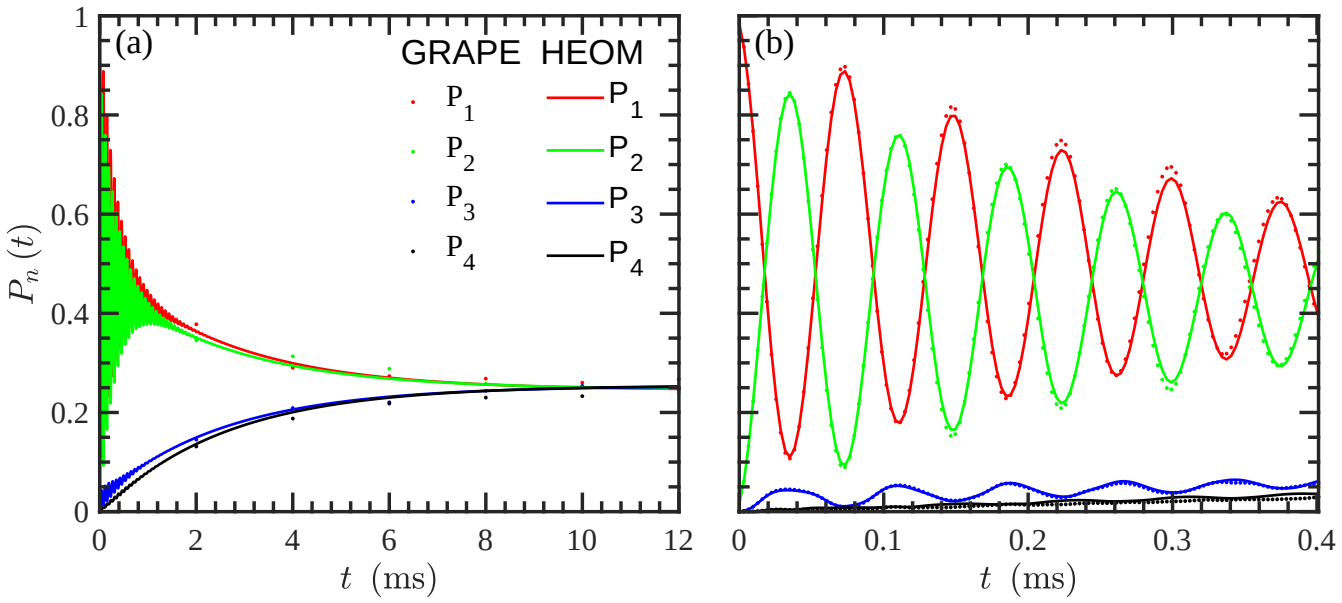

Figure S3. The symbols show the GRAPE results and the curves show the HEOM results. The time interval of (a) is $0 \sim 12$ ms, and the time of (b) interval is $0 \sim 0.5$ ms.

8. COMPUTATIONAL COSTS OF NMR AND HEOM

When the open quantum system consists of N levels or sites, each coupled to an independent bath (so N baths), and the correlation function of each bath contains K exponentials, there are [S9, S23]

$$\frac{(\mathcal{N}+KN)!}{\mathcal{N}!(KN)!} \leq \frac{\sqrt{2\pi}(\mathcal{N}+KN)^{\mathcal{N}+KN+\frac{1}{2}}e^{-(\mathcal{N}+KN)}}{e\mathcal{N}^{\mathcal{N}+\frac{1}{2}}e^{-\mathcal{N}}eKN^{KN+\frac{1}{2}}e^{-KN}} = \sqrt{\frac{2\pi(\mathcal{N}+KN)}{e^4\mathcal{N}KN}}\left(1+\frac{KN}{\mathcal{N}}\right)^{\mathcal{N}}\left(1+\frac{\mathcal{N}}{KN}\right)^{KN} \tag{S122}$$

density operators in a hierarchy with a cut-off of $\mathcal{N}$, where we have used the Stirling's formula [S19]. When the number of chlorophylls in the photosynthetic complex is very large, e.g. 96 chlorophylls in PSI and about 300 chlorophylls in PSII, and the form of the spectral density is complicated or the temperature is low,

$$\lim_{K,N\to\infty}\frac{(\mathcal{N}+KN)!}{\mathcal{N}!(KN)!} \leq \lim_{K,N\to\infty}\sqrt{\frac{2\pi(\mathcal{N}+KN)}{e^4\mathcal{N}KN}}\left(1+\frac{KN}{\mathcal{N}}\right)^{\mathcal{N}}\left(1+\frac{\mathcal{N}}{KN}\right)^{KN} = \sqrt{\frac{2\pi(\mathcal{N}+KN)}{e^4\mathcal{N}KN}}e^{\mathcal{N}+KN}. \tag{S123}$$

On the other hand, the computational cost of GRAPE is [S20, S21]

$$4^{\log_2 N} = N^2, \tag{S124}$$

where N is the number of energy levels involved in the energy transfer. Because the N-level photosynthetic light harvesting is simulated by $\log_2 N$-qubit NMR, the computational cost has the potential to be effectively reduced from exponential in N by the HEOM to polynomial in N by GRAPE.

9. EFFECT OF THE NUMBER OF RANDOM REALIZATIONS AND ERROR ANALYSIS

Errors are small and mainly caused by imperfections in the initial-ground-state preparation and GRAPE pulses, which can be estimated by numerical simulations. The remaining errors may originate from, e.g., imperfections in the experimental quantum control, the static magnetic field, and the spectral integrals.

As shown in Sec. 3, in the derivation of quantum dynamics under the influence of noise, we have assumed that the average over random realizations is equivalent to the average over time. The assumption is valid only if the number of random realizations M is in the infinite-M limit. In order to verify this assumption, we experimentally investigate the effect of number of random realizations on the NMR simulation, as shown in Fig. S4. As M increases from $M = 50$ to $M = 150$, the experimental

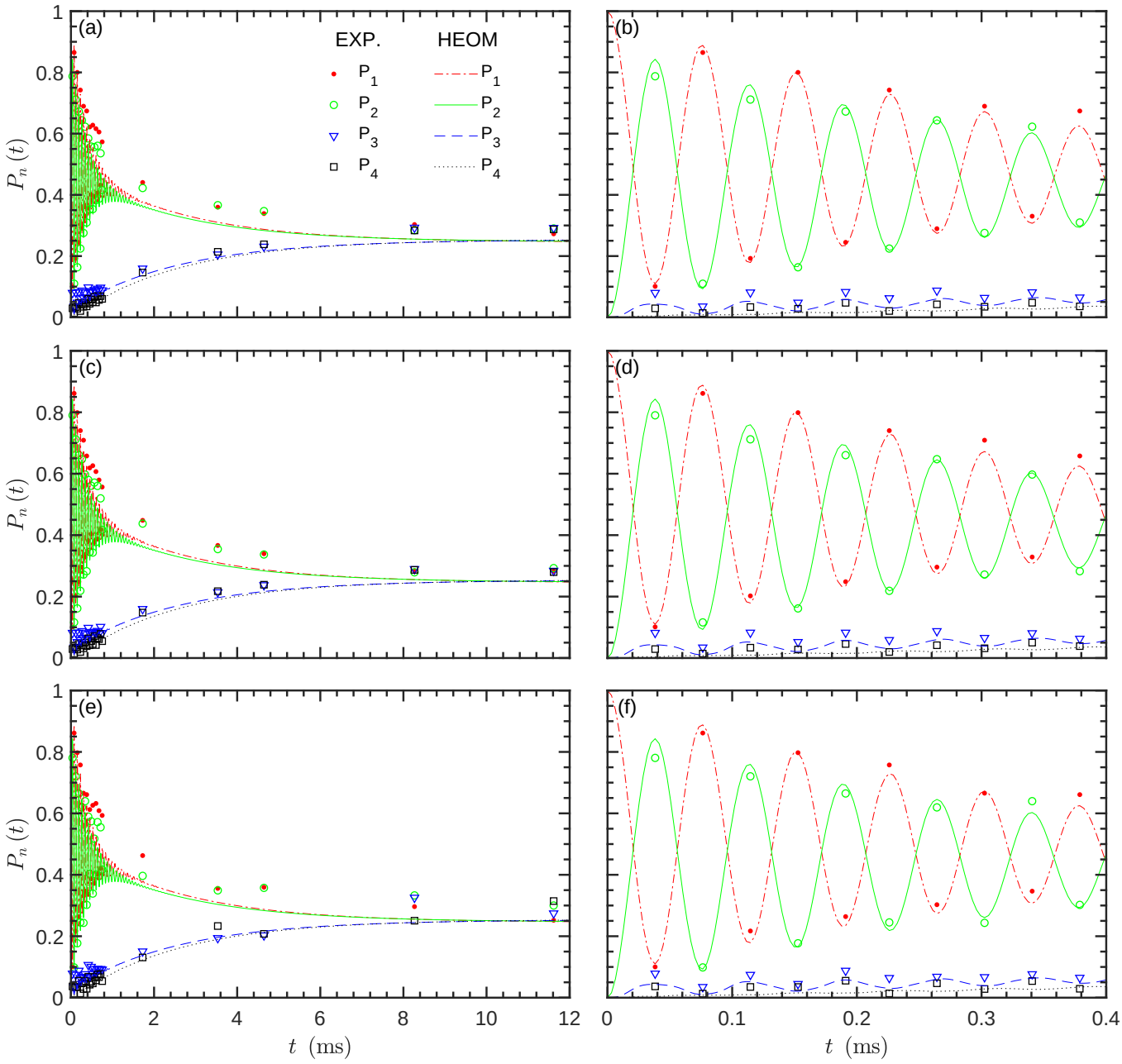

Figure S4. Simulation of the energy transfer governed by $H_{\rm NMR}$ for M random realizations: (a) and (b) $M = 50$, (c) and (d) $M = 100$, (e) and (f) $M = 150$. The right column is enlarged for short-time regimes in the left column. The symbols show the experimental data, and the curves are obtained from the numerical simulation using the HEOM.

simulation approaches closer and closer to the numerical simulation by the HEOM. In Fig. 4 of the main paper, we have compared the numerical results by GRAPE and HEOM for M =50, 500, and 5000. As M increases, the difference between the results by the GRAPE and the HEOM algorithms becomes smaller. When $M \sim 500$, the difference is hardly noticeable. Therefore, it is justified to mimic the photosynthetic energy transfer by the NMR with random realizations.

[S1] Cheng, Y.-C. & Fleming, G. R. Dynamics of light harvesting in photosynthesis. *Annu. Rev. Phys. Chem.* **60,** 241–262 (2009).

[S2] Lambert, N., Chen, Y.-N., Cheng, Y.-C., Chen, G.-Y. & Nori, F. Quantum biology. *Nature Phys.* **9,** 10–18 (2013).

[S3] Green, T. J., Sastrawan, J., Uys, H. & Biercuk, M. J. Arbitrary quantum control of qubits in the presence of universal noise. *New J. Phys.* **15**, 095004 (2013).

[S4] Soare, A. *et al.* Experimental bath engineering for quantitative studies of quantum control. *Phys. Rev. A* **89**, 042329 (2014).

[S5] Zhen, X.-L., Zhang, F.-H., Feng, G. R., Li, H. & Long, G.-L. Optimal experimental dynamical decoupling of both longitudinal and transverse relaxations. *Phys. Rev. A* **93,** 022304 (2016).

[S6] Sakurai, J. J. *Modern Quantum Mechanics* (Pearson Education, 2011).

[S7] Tanimura, Y. Stochastic Liouville, Langevin, Fokker-Planck, and master equation approaches to quantum dissipative systems. *J. Phys. Soc. Jpn.* **75,** 082001 (2006).

[S8] Ishizaki, A. & Fleming, G. R. Unified treatment of quantum coherent and incoherent hopping dynamics in electronic energy transfer: Reduced hierarchy equation approach. *J. Chem. Phys.* **130**, 234111 (2009).

[S9] Ishizaki, A. & Fleming, G. R. Theoretical examination of quantum coherence in a photosynthetic system at physiological temperature. *Proc. Natl. Acad. Sci. U.S.A.* **106,** 17255–17260 (2009).

[S10] Novoderezhkin, V. I. & van Grondelle, R. Physical origins and models of energy transfer in photosynthetic light-harvesting. *Phys. Chem. Chem. Phys.* **12**, 7352–7265 (2010).

[S11] Grabert, H., Schramm, P. & Ingold, G.-L. Quantum Brownian motion: The functional integral approach. *Phys. Rep.* **168**, 115–207 (1988).

[S12] Cory, D. G., Price, M. D. & Havel, T. F. Nuclear magnetic resonance spectroscopy: An experimentally accessible paradigm for quantum computing. *Phys. D* **120**, 82–101 (1998).

[S13] Lee, J.-S. The quantum state tomography on an NMR system, *Phys. Lett. A* **305**, 349–353 (2002).

[S14] Khaneja, N., Reiss, T., Kehlet, C., Schulte-Herbrüggen, T. & Glaser, S. J. Optimal control of coupled spin dynamics: design of NMR pulse sequences by gradient ascent algorithms. *J. Magn. Reson.* **172**, 296–305 (2005).

[S15] Blanes, S., Casas, F., Oteo, J. A. & Ros, J. The Magnus expansion and some of its applications. *Phys. Rep.* **470**, 151–238 (2009).

[S16] Goodman, J. W. *Statistical Optics* 2nd Ed. (Wiley, Hoboken, NJ, 2015).

[S17] Miller, S. L. & Childers, D. *Probability and Random Processes with Applications to Signal Processing and Communications* (Academic, Boston, MA, 2012).

[S18] Mukamel, S. *Principle of Nonlinear Optical Spectroscopy* (Oxford University Press, New York, 1995).

[S19] Robbins, H. A remark on Stirling's formula. *Am. Math. Mon.* **62**, 26–29 (1955).

[S20] Li, J., Yang, X. D., Peng, X. H. & Sun, C.-P. Hybrid quantum-classical approach to quantum optimal control. *Phys. Rev. Lett.* **118,** 150503 (2017).

[S21] Lu, D. W. *et al.* Quantum state tomography via reduced density matrices. *npj Quantum Inf.* **3,** 45 (2017).

[S22] Adolphs, J. & Renger, T. How proteins trigger excitation energy transfer in the FMO complex of green sulfur bacteria. *Biophys. J.* **91,** 2778–2797 (2006).

[S23] Shi, Q., Chen, L., Nan, G., Xu, R.-X. & Yan, Y. J. Efficient hierarchical Liouville space propagator to quantum dissipative dynamics. *J. Chem. Phys.* **130,** 084105 (2009).